Journal of the European Ceramic Society 16 (1996) 715–719

0955-2219(95)00205-7
0955-2219/96/$15.00

Thermal Shock Behaviour of Si_3N_4/SiC Composites

A. Kaiser, R. Vaßen & D. Stöver

Institut für Werkstoffe der Energietechnik Forschungszentrum Jülich GmbH KFA, 52425 Jülich, Germany

(Received 15 July 1995; revised version received 6 November 1995; accepted 13 November 1995)

Abstract

In the present study the thermal shock behaviour of Si_3N_4/SiC composites with and without Y_2O_3 as additive was investigated using the KFA electron beam test facility JUDITH at energy densities of up to 9 MJ m^{-2}, which is designed for disruption simulations of materials for the first wall of a fusion reactor. The influence of SiC content, microstructure, additive and density on thermal shock behaviour and mass loss is discussed. Composites with additive have a slightly higher mass loss rate, but show no catastrophical thermal shock behaviour as do the composites without additives. Samples with lower density in the system with additive revealed no visible difference in mass loss and fracture behaviour.

1 Introduction

Most investigations on the properties of Si_3N_4 concern optimization of the fracture toughness K_{IC} and bending strength, but Si_3N_4 also exhibits good corrosion resistance and thermal shock resistance. Si_3N_4 powder without additive can only be densified by hot-isostatic pressing (HIP) and the resulting dense specimens have good oxidation resistance because of the low amount of the silica grain-boundary phase.[1] But the microstructure consists of equiaxed grains and these samples therefore have relatively low values of K_{IC}. It is well known that using sintering agents leads to the self-reinforcement of Si_3N_4 during sintering via the formation of a needle-like structure, and fracture toughness is increased.[2] The oxidation resistance is more or less significantly reduced, depending on the additive system used, because of the higher amount of glassy phase.[1] It is therefore of interest to study the influence of additives as a secondary phase and microstructure (i.e. grain morphology) on the thermal shock behaviour. When SiC was added to the system Si_3N_4/additive the needle-like structure was changed and almost equiaxed grains appeared,[3] as is known for Si_3N_4/SiC without additives,[4] and thus the influence of additive on the thermal shock behaviour can be elucidated.

2 Experimental

2.1 Processing and sample characterization

Mixtures of α-Si_3N_4 (450 nm) with 10 and 20 wt% β-SiC (500 nm), both supplied by H. C. Starck Germany, or nanosized β-SiC (20 nm)[5] and 8 wt% Y_2O_3, also supplied by H. C. Starck, were used as starting materials. HIPing of these powders using quartz capsules at temperatures of 1750–1800°C for composites with Y_2O_3 and 1900°C for the Si_3N_4/SiC system and pressures of 200 MPa, respectively, resulted in compacts with densities >98% of theoretical density.[3,4]

The microstructure of Si_3N_4/SiC/Y_2O_3 revealed a bimodal grain size distribution of Si_3N_4 grains, with equiaxed micrometre-sized α- and β-Si_3N_4 grains (2–4 μm) surrounding larger needle-like β-Si_3N_4 grains. Aspect ratios up to 10 were found. The amount of equiaxed grains increased with higher SiC contents, because SiC particles suppressed the phase transformation of α- to β-Si_3N_4. Transmission electron micrographs of Si_3N_4/10% SiC/8% Y_2O_3 indicated that nanometre-sized SiC particles were uniformly dispersed in the Si_3N_4 matrix as well as along the grain boundaries. The majority of grain boundaries seemed to be free of any second phase. The additive was predominantly located as amorphous phase in triple points at the grain-boundary junctions. The grain boundary phase consisted of $Y_2O_3{\cdot}SiO_2$, $Y_2Si_2O_7$ and $Y_5N(SiO_4)_3$. These were formed by a reaction of Y_2O_3 and SiO_2 or Si_3N_4, with silica coming from the surfaces of Si_3N_4 and SiC.

Equiaxed Si_3N_4 grains with average grain sizes of 1·5 μm were found in the case of Si_3N_4/SiC composites. In the case of addition of nano-SiC, nanometre-sized SiC particles are believed also to be found inside Si_3N_4 grains as in the case of composites with Y_2O_3.

Vickers hardness H_v10 of Si_3N_4/SiC composites[4] increased from 15·5 to 18 GPa, and in the case of

composites with Y_2O_3[3] from 14 to 16 GPa, with increasing SiC content. Hardness was decreased by the addition of Y_2O_3 because of the glassy structure of the grain-boundary phase. Fracture toughness K_{Ic} of the composites, measured by the indentation technique, was nearly independent of SiC content. If Y_2O_3 was used as an additive fracture toughness increased from 3·5 to 6·5 MPa $m^{1/2}$. The grain boundaries are weakened by the additive and the appearance of crack deflection is intensified.

2.2 Thermal shock tests

Thermal shock tests were performed with electron beam loadings in the JUDITH facility with energy densities of 2·3, 4·5 and 9·1 MJ m^{-2} and pulse duration of 3 ms. The acceleration voltage was 120 kV and the size of the scanned beam was 3 × 3 mm^2. Mass loss decreases strongly after the first pulse and after 5 pulses is nearly constant. Therefore 10 pulses were applied and the averaged mass loss per pulse was determined. Specimens had a diameter of about 8 mm and a height of 4 mm. During thermal shock at the JUDITH facility the surface is heated to temperatures close to 3000°C[6] and thermal stresses arise.

A model to calculate the erosion rates of weight loss is presented in Refs 6 and 7, and is very briefly described here. This model is based on the equivalence of the different energy density currents, i.e. the incoming energy density j_Q is compensated by several outgoing energy density currents:

$$j_Q = j_{sub} + j_{rad} + j_\lambda + j_{cp} + j_m \qquad (1)$$

with j_{sub} and j_{rad} as the energy density currents due to sublimation and radiation from the surface. j_λ describes the heat current into the sample by thermal conductivity. The electrons penetrate into the solid and heat up a surface layer with a given heat capacity c_p. This energy current is described by j_{cp}. During the heating phase the erosion rate dm/dt is determined by the sublimation term j_{sub}. After reaching a critical temperature, which corresponds to the maximum compression stress the sample is able to sustain,[7] the heating rate is set equal to zero and the energy balance is now achieved by an additional term, j_m. This term, $j_m = c_p \rho T\, dm/dt$ with ρ the density of the sample and T the temperature, decribes the energy required to heat up the cooler parts of the sample after erosion of hot surface elements. Creep can be introduced into the model by simply reducing the thermal expansion by the integrated creep rate. Reduction of surface stress by creep reduces particle erosion (j_m) and increases surface temperature. This leads to an increase of the sublimation rate and a reduced erosion rate, because sublimation consumes more energy than the mechanism described by j_m.

This model will serve as an aid to explain the effects of decomposition temperature, thermal conductivity and compression strength on the erosion rates, but can give no information about the thermal shock behaviour.

In the theory developed by Hasselmann *et al.*,[8] catastrophic crack propagation caused by thermal shock is reduced by maximizing the parameter

$$R'''' = NGE/\sigma_f^2 \qquad (2)$$

with N as the number of cracks nucleated during fracture, G as the fracture energy expended in creating unit area of new fracture surface, E as the Young's modulus and σ_f as the fracture stress. Using the equation of Griffith ($\sigma_f \approx K/\sqrt{a}$) and with the fracture energy $G \approx K^2/E$ gives

$$R'''' \approx a \qquad (3)$$

with a as the defect size. This parameter R'''' will serve to explain recent thermal shock behaviour.

3 Results and Discussion

3.1 Results

3.1.1 System without additive

In Table 1 results of JUDITH tests of the system Si_3N_4/SiC are summarized. No sample could bear the energy density of 9·1 MJ m^{-2}, even for one pulse. This high energy led to breakage of the samples into many small and larger pieces. Mass loss of these samples could not be determined because not all small parts of one broken sample, which were widely spread in the large vacuum chamber of the JUDITH facility, could be found after the experiment.

3.1.2 System with additive

Figure 1 shows the mass losses of Si_3N_4/SiC/Y_2O_3 systems for various energy densities, while Fig. 2 reveals the influence of density on mass losses of the same systems for various energy densities. At 2·3 MJ m^{-2} sometimes high values of mass losses

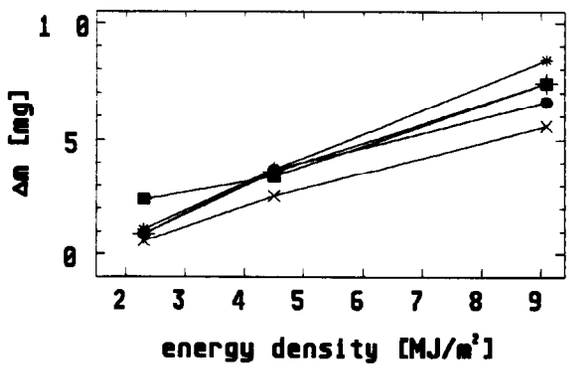

Fig. 1. Averaged mass losses after test in JUDITH facility of composites with 8 wt% Y_2O_3: X; Si_3N_4 (98·1%); ■, Si_3N_4/10% HCS-SiC (97·9%); ●, Si_3N_4/20% HCS-SiC (98·3%); +, Si_3N_4/10% nano-SiC (97·9%); *, Si_3N_4/20% nano-SiC (98·1%).

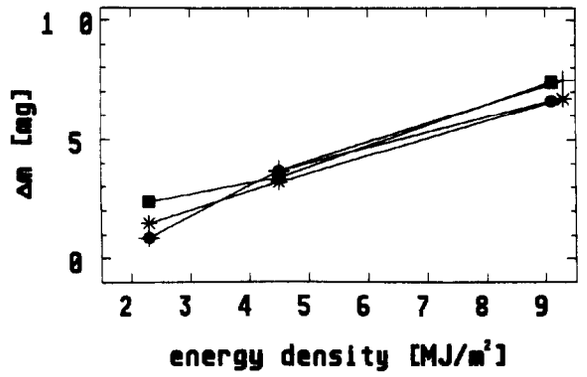

Fig. 2. Averaged mass losses after test in JUDITH facility of composites with 8 wt% Y_2O_3 and different densities: ■, Si_3N_4/10% HCS-SiC (97·9%); ●, Si_3N_4/20% HCS–SiC (98·3%); +, Si_3N_4/10% HCS-SiC (85·9%); *, Si_3N_4/20% HCS-SiC (93·8%).

were found (Figs 1 and 2: ■). This effect was attributed to breaking off of larger particles, which increased mass loss significantly especially at low averaged mass losses found at low energies.

3.2 Discussion

3.2.1 System without additive

Mass loss increased with increasing energy density in the system Si_3N_4/SiC (Table 1). At the energy density of 2·3 MJ m^{-2} all samples showed no difference in mass loss, whereas mass loss at an energy density of 4·5 MJ m^{-2} was decreased if SiC was added. The explanation of this effect is the higher decomposition temperature (j_{sub}) and higher thermal conductivity (j_λ) of SiC. This is also indicated by the lower mass loss rate of pure SiC[6] compared with pure Si_3N_4 of these results. Because of the energy balance higher terms of j_{sub} and j_λ lead to a lower term j_m, thus giving a lower erosion rate. Additionally, the higher compression strength of SiC compared with Si_3N_4 leads to a higher critical temperature (see section 2.2) and a longer time, when sublimation (j_{sub}) determines mass loss. Lower values of dm given by j_{sub} than by the term j_m (see section 2.2) result in a decrease of mass loss with higher compression strength.

Residual stress because of thermal mismatch between SiC and Si_3N_4 after sintering will lead to

Table 1. Averaged mass losses (mg) after 10 pulses in the JUDITH facility for the Si_3N_4/SiC-system (* indicates mass loss for one pulse)

	Energy (mJ m^{-2})	
System	*2·3*	*4·5*
Si_3N_4	1·1	5·1
Si_3N_4+10% HCS-SiC	0·9	3·1
Si_3N_4+20% HCS-SiC	1·1	2·0
Si_3N_4+10% nano-SiC	1·0	3·1
Si_3N_4+20% nano-SiC	—	<3·0*

Fig. 3. SEM micrograph of Si_3N_4/10 wt% nano-SiC after 2·3 MJ m^{-2}: the bar indicates 100 μm; ← beam direction.

an increased number of nucleation centres of thermal fracture and therefore to a higher crack density and additional energy absorption. Figure 3 shows a micrograph of the transition zone of the loaded region to the bulk Si_3N_4/10 wt% nano-SiC after a JUDITH test. In the system Si_3N_4/SiC cracks parallel to beam direction were found. These cracks were responsible for the catastrophic behaviour of this system. At higher energy densities the tensile thermal stress at the disc edge was too high and led to the growth of cracks through the samples and consequent breakage.

No visible influence of SiC content or SiC powder on the fracture behaviour was found, probably because of the small resolution of energy density. More experiments with energy densities between 4·5 and 9·1 MJ m^{-2} should give more information.

3.2.2 System with additive

In the system Si_3N_4/SiC/Y_2O_3 the addition of SiC led to an increase of mass loss (Fig. 1). No dependence of SiC content or type of SiC powder on mass loss could be found. Si_3N_4/Y_2O_3 has the most pronounced needle-like structure and no preferred direction of the elongated grains exists. The elongated grains improve the thermal conductivity[9] compared with an equiaxed structure, which has a higher amount of grain boundaries. This leads to a higher j_λ term and therefore a lower erosion rate, given by the term j_m, is reached. This overcompensates the positive effect of SiC on j_{sub} and j_λ and of higher compression strength on mass loss (see section 3.2.1). Figure 4 shows a micrograph of the transition of the loaded region to the bulk Si_3N_4/10 wt% nano-SiC/8 wt% Y_2O_3 after a JUDITH test. No cracks as they exist in the system Si_3N_4/SiC were found. In this system a small layer at the surface within the loaded region broke off the bulk. The high temperature during the JUDITH test leads to weakening of the grain-boundary

phase, especially in the case of samples with additives. Therefore small layers exist at the surface with weakened grain boundaries, while in the inner regions the temperature is lower than the melting point of the grain-boundary phase and interface strength is higher. Cracks are favoured to propagate in the direction of the weak grain boundaries parallel to the surface.

Assuming a similar distribution of defect size [eqn. (3)] in samples with and without additive, no improvement in thermal shock behaviour is reached. The positive effect of the grain-boundary phase Y_2O_3 to the thermal shock behaviour of Si_3N_4/SiC/additive is explained by the higher creep rate of samples with additive,[10] which decreases the thermal stress, and the lower Young's modulus of the grain-boundary phase as the second phase, leading to a high *E*/low *E* composite with improved thermal shock behaviour.[8,11] Also, the higher number *N* of nucleated cracks in Si_3N_4/SiC/Y_2O_3 samples has to be regarded. In the system with additive grain boundaries are weaker than without additive, especially at high temperatures. Therefore crack initiation is favoured and *N* is increased.

Samples with and without SiC were also tested at the highest possible energy density of 22·3 MJ m^{-2}. All samples survived. Therefore no statement about the influence of SiC on the fracture behaviour can be made.

Figure 2 shows the mass losses of Si_3N_4 with 10 and 20% HCS-SiC with Y_2O_3 for different densities (94 and 86%) and various energy densities. Mass loss increased with increasing energy density, but there were no significant differences found between dense and porous samples. In Ref. 12 even smaller mass losses were found for samples made of SiC/B_4C/C, if they had lower density (ρ = 75%). This effect is currently not understood, because it is difficult to describe the dependence of mass loss on microstructure, but it will be taken into consideration in the model. Pores in samples with lower density can be regarded as second phase with lower Young's modulus, leading to better thermal shock behaviour.[8] A higher density of pores increases the number *N* of nucleated cracks [eqn (2)]. Also, larger pores in porous samples increase R''' [eqn (3)]. However, due to limitations of the test facility, energy density could not be further increased to reveal a different behaviour of dense and porous samples.

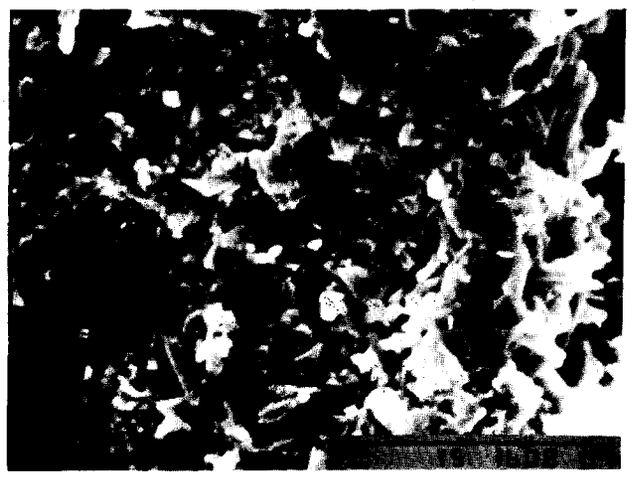

Fig. 4. SEM micrograph of Si_3N_4/10 wt% nano-SiC/8 wt% Y_2O_3 after 4·5 MJ m^{-2}: the bar indicates 10 μm; ← beam direction.

4 Summary

Si_3N_4/SiC composites with 10 and 20 wt% HCS- or nano-SiC with and without Y_2O_3 as additive were tested by the KFA electron beam test facility at energy densities of up to 9·1 MJ m^{-2}. The system Si_3N_4/SiC breaks catastrophically at energy densities of 9·1 MJ m^{-2}, while in the system with Y_2O_3 addition no such cracks were formed. The positive effect of Y_2O_3 on the thermal shock behaviour is explained by the effect of microstructure and high(Si_3N_4/SiC)/low(Y_2O_3) modulus composites. SiC decreases the mass loss in the system Si_3N_4/SiC and increases mass loss in the system Si_3N_4/SiC/Y_2O_3.

Acknowledgements

The authors thank Dr Förster, Institut für Laser und Plasmaphysik, Universität Düsseldorf, for producing the ultrafine SiC powder; Mr Coenen and Mr Gelissen, our Institute, for assisting this work and the other members of the Forschungszentrum Jülich who contributed to the present work; Dr Duwe and Mr Münstermann, Heiße Zellen (HZ), for performing the JUDITH tests; Mr. D'Orsaneo and his colleagues, Zentralabteilung Technologie (ZAT), for the preparation of quartz capsules.

References

1. Jacobson, N. S., Corrosion of silicon-based ceramics in combustion environments. *J Am. Ceram. Soc.*, **76** (1993) 3–28.
2. Wötting, G., Gugel, E., Schwier, G. & Lange, H., Processing for improved fracture toughness of dense silicon nitride. In *Ceramic Powder Science IV, Ceram. Trans. vol. 22*, ed. S. Hirano, G. L. Messing & H. Hausner. The American Ceramic Society, Inc., Westerville, OH, 1989, pp. 647–54.
3. Kaiser, A., Vaßen, R., Stöver, D., Buchkremer, H. P. & Kesternich, W., Composites of Si_3N_4 and nanosized SiC. To be published in *Silicates Industriels, Proceedings of Ceramic Ceramic Composites III*, Mons, October 1994.

4. Kaiser, A., Vaßen, R., Stöver, D., Buchkremer, H. P., Förster, J. & Uhlenbusch, J., Si_3N_4 SiC composites using conventional and nanosized powders. *Nanostructured Mater.*, **6** (1995) 917–20.
5. Förster, J., Hoesslin, M. v., Schäfer, J. H., Uhlenbusch, J. & Viöl, W., Optimization of CO_2 laser assisted synthesis of ultrafine silicon and silicon carbide powders. In *Proceedings of the 10th International Symposium on Plasma Chemistry*, Bochum, Germany, 1991, pp. 1–6.
6 Vaßen, R., Förster, J., Yehia, A., Hammelmann, K., Buchkremer, H.-P., Bolt, H. & Stöver, D., Development of low-Z materials for plasma facing, structural applications in fusion reactors. In *Proceedings of the 18th Symposium on Fusion Technology*, Karlsruhe, 1994, Elsevier Science BV, The Netherlands, pp. 259–62.
7. Vaßen, R., Kaiser, A. & Stöver, D., Potential of nanocrystalline low-Z materials for plasma facing, structural application in fusion reactors. To be published in *J. Nuclear Mater.*, 1995.
8. Hasselmann, D. P. H., Becher, P. F. & Mazdiyasni, K. S., Analysis of the resistance of high-E, low-E brittle composites to failure by thermal shock. *Z. für Werkstofftechnik*, **11** (1980) 82–92.
9. Ziegler, G., Thermal properties and thermal shock resistance of silicon nitride. In *Progress in Nitrogen Ceramics*, ed. F. L. Riley. Martinius Nijihoff Publisher, The Netherlands, 1983, pp. 565–88.
10. Hvidos, P. & Dusza, J., Deformation and fracture behaviour of two Si_3N_4 ceramics with different sintering additives. *Scripta Metall. Mater.*, **32** (1995) 1459–64.
11. Mazdiyasni, K. S. & Ruh, R., High/low modulus Si_3N_4–BN composite for improved electrical and thermal shock behaviour. *J. Am. Ceram. Soc.*, **64** (1981) 415–19.
12. Yehia, A., Vaßen, R., Duwe, R. & Stöver, D., Ceramic SiC/B_4C/TiC/C composites as plasma facing components for fusion reactors. To be published in *J. Nuclear Mater.*, 1995.